Journal of Advanced Research in Applied Sciences and Engineering Technology

Journal homepage:
https://semarakilmu.com.my/journals/index.php/applied_sciences_eng_tech/index
ISSN: 2462-1943

Numerical Scheme by Legendre-Galerkin for Characterization of Micropolar-Maxwell Unsteady Fluid Model

Khaled M Abdelgaber[1,*], Mohamed Fathy[2]

[1] Department of Physics & Engineering, Mathematics, Faculty of Engineering - Mataria, Helwan University, Cairo, Egypt
[2] Basic and Applied Science Department, College of Engineering and Technology, Arab Academy for Science, Technology and Maritime Transport, Cairo, Egypt

ARTICLE INFO

Article history:
Received 10 October 2023
Received in revised form 19 December 2023
Accepted 24 March 2024
Available online 25 April 2024

Keywords:

Stretching sheet; Micropolar fluid; Legendre; Galerkin; Maxwell fluid; Magnetic field

ABSTRACT

In this paper, Micropolar-Maxwell unsteady fluid flow prior an expanding sheet is asymptotically investigated using an efficient Legendre-Galerkin technique in the existence of magnetic field. By employing fitting similarity mapping to the controlling partial differential equations, a system of nonlinear ordinary differential equations is obtained. In comparison to the prior studies, the suggested asymptotic outcomes are guaranteed. The impacts of elasticity/material parameters on velocity/micro-rotation profiles are shown and explored with the help of tables and figures to enhance the mechanical properties of the sheet.

1. Introduction

It is common practice to use non-Newtonian fluid cooling fluids like polymeric melts and solutions in the production of adhesive tapes, hot winding processes, glass blasting, and plastic surfaces. Figure 1 depicts the flow of melting fluid through a quiescent fluid at a constant speed after it is extruded from a die. An electromagnetic field is used to perform the procedure. Using a wind-up roll, the sheet is rolled into the desired shape after it has cooled. Many high-cost metallurgical applications, polymer extrusion processes, and chemical manufacturing processes make use of this technique. The primary purpose of this technique is to enhance the mechanical characteristics of the ultimate product. This may be accomplished by adjusting the cooling rate, the natural parameters of the cooling surrounding, like heat conduction, affecting the cooling rate, and the viscosity of the liquid. This determines the amount of drag necessary to pull the sheet. The depth of the boundary layer and the coefficient of friction of the skin across the stretched sheet are governed by the velocity of the stretched web and the physical characteristics of the cooling medium [1].

* *Corresponding author.*
E-mail address: khaled.abdelgaber@m-eng.helwan.edu.eg

https://doi.org/10.37934/araset.44.1.94104

Using electrically conductive fluids and a magnetic field, the MHD flow has recently been employed in petroleum and metallurgical processes to manage the qualities of the product. The magnetic field has been utilized to pacificate non-metallic contaminants from molten metals [2]. Many researchers have lately studied that sort of flow to forecast the force needed to draw these surfaces. Starting with the Cauchy equations of motion, Maxwell fluid defines the hard impacts of viscidity, elasticity, and diverse features on the boundary layer of a viscoelastic fluid [3-9]. The chemical reaction on the Maxwell fluid takes place in conjunction with the magnetic field [10,11]. As an alternative, micro-polar fluids theory depicts fluids with microscopic features. Suspended particles (at most spherical in shape) may be found in viscous media if deformation is not considered. Complex fluids may now be modelled in a few applications by the modified Navier-Stokes equation [12-16]. Advances in the research of fluid flow/heat transfer are made by a lot of researchers [17-19].

When a surface in a transverse magnetic field is being stretched, an asymptotic study of the micropolar effect and elasticity parameter effect is presented in this dissertation. To provide an asymptotic evaluation of the problem, the Legendre-Galerkin technique is used. There are graphs showing the impacts of varying the magnetic, elasticity, and micro-polar on the skin friction and micro-rotation profiles, as well as tables listing the results.

2. Mathematical Formulation

In a Maxwell fluid, consider an unsteady laminar boundary layer flow of micro-polar fluid across an expanding surface in of two-dimensional space. The exterior is stretched by the velocity $U_w = bx$ and is accepted to be impermeable, $V_w = 0$. The x-axis is selected parallel to the expanding exterior in the motion's course and the y-axis is chosen perpendicular to it. Figure 1 illustrates the flow layout. Also, the stretching surface is subjected to a normal uniform magnetic field B_o. The induced magnetic field is ignored since the magnetic Reynolds number is negligible. The stream is governed by [12]:

$$\frac{\partial u}{\partial x} + \frac{\partial v}{\partial y} = 0, \tag{1}$$

$$\frac{\partial u}{\partial t} + u\frac{\partial u}{\partial x} + v\frac{\partial v}{\partial y} + \lambda\left[u^2\left(\frac{\partial^2 u}{\partial x^2}\right) + v^2\left(\frac{\partial^2 u}{\partial y^2}\right) + 2uv\left(\frac{\partial^2 u}{\partial x \partial y}\right)\right] = \left(\nu + \frac{s}{\rho}\right)\frac{\partial^2 u}{\partial y^2} + \frac{s}{\rho}\frac{\partial N}{\partial y} - \frac{\sigma B_o^2}{\rho}u, \tag{2}$$

$$\frac{\partial N}{\partial t} + u\frac{\partial N}{\partial x} + v\frac{\partial N}{\partial y} = \left(\frac{\gamma}{\rho j}\right)\frac{\partial^2 N}{\partial y^2} - \frac{s}{\rho j}\left(2N + \frac{\partial u}{\partial y}\right), \tag{3}$$

given that u and v are the components of velocity along x and y, respectively.

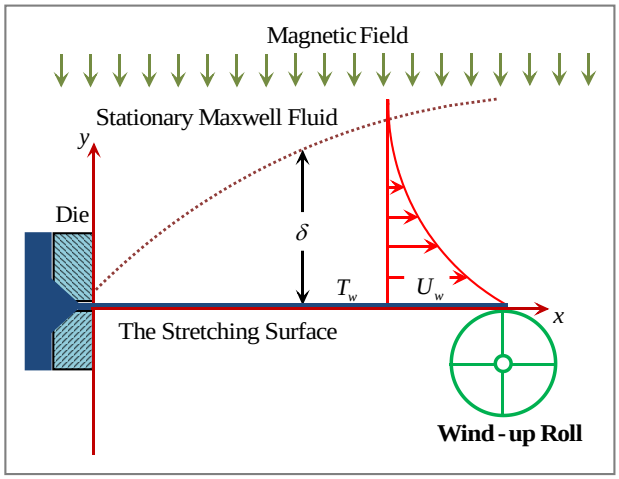

Fig. 1. Schematic for flow above stretching surface

Microrotation is denoted by N, the magnetic field by B_o, the relaxation time by λ, the vortex by s, and the electrical conductivity by σ. The fluid parameters are symbolized by ρ for density, ν for dynamic viscosity, j for micro-inertia per unit mass, γ for spin gradient, and t for time. For $t > 0$, the governing equations are subjected to:

$$u = U_w, \quad v = 0, \quad N = -n\frac{\partial u}{\partial y} \quad \text{if} \quad y = 0 \quad \text{and} \quad \lim_{y\to\infty} u = \lim_{y\to\infty} N = 0, \tag{4}$$

3. Transformation Based on Similarity

To satisfy the equation of continuity, it must be possible to choose an appropriate stream function ψ such that $u = \partial\psi/\partial y$ and $v = -\partial\psi/\partial x$. Dimensionless similarity variables

$$\eta = \sqrt{\frac{b}{\nu\zeta}}y, \ \zeta = 1 - e^{-bt}, \ \psi = x\sqrt{b\nu\zeta}\, f(\eta,\zeta), \ N = bx\sqrt{\frac{b}{\nu\zeta}}g(\eta,\zeta), \tag{5}$$

$$u = xbf'(\eta,\zeta), \ v = -\sqrt{b\nu\zeta}f(\eta,\zeta). \tag{6}$$

and the linear transformation $\eta = \eta_\infty(\xi + 1)/2$ are used to simplify the system Eq. **Error! Reference source not found.** to Eq. **Error! Reference source not found.** and to convert the solution domain from $[0, \eta_\infty]$ to $[-1, 1]$. The new system format of the system Eq. **Error! Reference source not found.**to Eq. **Error! Reference source not found.** is:

$$\frac{8}{\eta_\infty^3}(1+K)\,f''' + \frac{1}{\eta_\infty}(1-\zeta)(\xi+1)f'' + \frac{4}{\eta_\infty^2}\zeta\left(ff'' - f'^2 - \frac{\eta_\infty}{2}Mf'\right) + \frac{2}{\eta_\infty}Kg' + \frac{8}{\eta_\infty^3}\zeta\beta(2ff'f'' - f^2f''') = 0, \tag{7}$$

$$\frac{1}{\eta_\infty^2}(4+2K)g'' + (\xi+1)(g + (1-\zeta)g') + \frac{2}{\eta_\infty}\zeta(fg' - f'g) - 2K\zeta g - \frac{4}{\eta_\infty^2}K\zeta f'' = 0, \tag{8}$$

with the following conditions:

$$f(-1) = 0, \quad f'(-1) = \frac{\eta_\infty}{2}, \quad g(-1) = -\frac{4n}{\eta_\infty^2}f''(-1), \quad f'(1) = 0, \quad g(1) = 0. \tag{9}$$

where $\beta = \lambda b$ is the elasticity number, $M = \sigma B_o^2/\rho$ is the magnetic parameter, $K = s/\rho v = s/\mu$ is the material parameter and $j = v/b$ is micro-inertia per unit mass. Skin friction coefficient

$$C_f = \frac{2\tau_w}{\rho U_w} = \left[(\mu + \lambda b + s)\frac{\partial u}{\partial y} + sN\right]_{y=0}$$

is transformed to be $C_f\sqrt{\mathrm{Re}_x} = -\zeta^{-0.5}(1 + \beta + (1-n)K)f''(0)$, where τ_w is the shear stress and $\mathrm{Re}_x = \rho U_w x/\mu$ is the local Reynold number.

4. Solution Proceeding

Combining Eq. **Error! Reference source not found.** to Eq. **Error! Reference source not found.**, the problem is solved asymptotically using Legendre-Galerkin Method. The asymptotic solutions, $f(\xi)$ and $g(\xi)$, are assumed as series in the Legendre polynomials $P_i(x)$, i.e., $f(\xi) \approx \sum_{i=0}^{m} c_i\, P_i(\xi)$ and $g(\xi) \approx \sum_{i=0}^{m} d_i\, P_i(\xi)$. When they are substituted into the Eq. (12) and Eq. (15) and the Galerkin technique is used, the result is

$$\sum_{j=0}^{m} c_j \left[\langle \frac{8}{\eta_\infty^3}(1+K)P_j'''(\xi) + \frac{1}{\eta_\infty}(1-\zeta)P_j''(\xi) - \frac{1}{\eta_\infty}(1-\zeta)\xi P_j''(\xi) - \frac{2M}{\eta_\infty}P_j'(\xi), P_r(\xi)\rangle\right]$$
$$+\frac{2K}{\eta_\infty}\sum_{i=0}^{m} d_i\langle P_j'(\xi), P_r(\xi)\rangle + \frac{4\zeta}{\eta_\infty^2}\sum_{j=0}^{m}\sum_{i=0}^{m} c_j c_i\left[\langle P_i(\xi)\, P_j''(\xi) - P_i'(\xi)P_j'(\xi), P_r(\xi)\rangle\right]$$
$$+\frac{8\zeta\beta}{\eta_\infty^3}\sum_{j=0}^{m}\sum_{i=0}^{m}\sum_{k=0}^{m} c_j c_i c_k\left[2\langle P_i(\xi)P_j''(\xi)P_j'(\xi), P_r(\xi)\rangle - \langle P_i(\xi)P_j(\xi)P_j'''(\xi), P_r(\xi)\rangle\right] = 0,$$
$$\sum_{j=0}^{m} d_j\left[\langle \frac{1}{\eta_\infty^2}(4+2K)P_j''(\xi) + P_j(\xi) + \xi P_j(\xi) + (1-\zeta)\left(P_j'(\xi) + \xi P_j'(\xi)\right) + 2K\zeta P_j(\xi), P_r(\xi)\rangle\right] \quad (10)$$

$$-\frac{4K\zeta}{\eta_\infty^2}\sum_{j=0}^{m} c_j\,\langle P_j''(\xi), P_r(\xi)\rangle + \frac{2\zeta}{\eta_\infty}\sum_{j=0}^{m}\sum_{i=0}^{m} d_j c_i\,\langle P_i(\xi)P_j'(\xi) - P_j(\xi)P_i'(\xi), P_r(\xi)\rangle = 0, \quad (11)$$

with boundary conditions:

$$\sum_{i=0}^{m}(-1)^j\, c_i = 0, \quad \sum_{i=0}^{m}(-1)^j\frac{j(j+1)}{2}c_i = \frac{\eta_\infty}{2}, \quad \sum_{i=0}^{m}\frac{j(j+1)}{2}c_i = 0, \quad \sum_{i=0}^{n} d_j = 0,$$
$$\sum_{i=0}^{m}(-1)^j\left[d_j + \frac{n}{2\eta_\infty^2}c_i\prod_{o=-1}^{2}(i+o)\right] = 0 \quad (12)$$

where the inner product is determined by $\langle \Upsilon(\xi),\ \chi(\xi)\rangle = \int_{-1}^{1}\Upsilon(\xi)\ \chi(\xi)\ d\xi$. The nonlinear system Eq. **Error! Reference source not found.** to Eq. **Error! Reference source not found.** can be represented in matrix form

$$\mathbf{\Lambda c} + \mathbf{\Phi}\tilde{\mathbf{c}} + \mathbf{\Theta}\bar{\mathbf{c}} + \mathbf{\Gamma}\check{\mathbf{c}} = \mathbf{b}, \quad (13)$$

where:

$$\boldsymbol{\Lambda} = \begin{pmatrix} \boldsymbol{\Lambda}_{11} & \boldsymbol{\Lambda}_{12} \\ \boldsymbol{\Lambda}_{21} & \boldsymbol{\Lambda}_{22} \end{pmatrix}, \quad \boldsymbol{\Phi} = \begin{pmatrix} \boldsymbol{\Phi}_{\mathbf{f}} \\ \mathbf{O} \end{pmatrix}, \quad \boldsymbol{\Theta} = \begin{pmatrix} \boldsymbol{\Theta}_{\mathbf{f}} \\ \mathbf{O} \end{pmatrix}, \quad \boldsymbol{\Gamma} = \begin{pmatrix} \mathbf{O} \\ \boldsymbol{\Gamma}_{\mathbf{f}} \end{pmatrix}, \quad \mathbf{b} = \begin{pmatrix} \mathbf{b_1} \\ \mathbf{b_2} \end{pmatrix},$$

$$\boldsymbol{\Lambda}_{11} = \begin{pmatrix} \omega_{0,0} & \omega_{0,1} & \cdots & \omega_{0,m-1} & \omega_{0,m} \\ \omega_{1,0} & \omega_{1,1} & \cdots & \omega_{1,m-1} & \omega_{1,m} \\ \vdots & \vdots & \vdots & \vdots & \vdots \\ \omega_{m-3,0} & \omega_{m-3,1} & \cdots & \omega_{m-3,m-1} & \omega_{m-3,m} \\ 1 & -1 & \cdots & (-1)^{m-1} & (-1)^{m} \\ 0 & 1 & \cdots & (-1)^{m} m(m-1) & (-1)^{m+1} m(m+1) \\ 0 & 1 & \cdots & m(m-1) & m(m+1) \end{pmatrix},$$

$$\boldsymbol{\Lambda}_{12} = \begin{pmatrix} \epsilon_{0,0} & \epsilon_{0,1} & \cdots & \epsilon_{0,m} \\ \epsilon_{1,0} & \epsilon_{1,1} & \cdots & \epsilon_{1,m} \\ \vdots & \vdots & \vdots & \vdots \\ \epsilon_{m-3,0} & \epsilon_{m-3,1} & \cdots & \epsilon_{m-3,m} \\ 0 & 0 & \cdots & 0 \\ 0 & 0 & \cdots & 0 \\ 0 & 0 & \cdots & 0 \end{pmatrix}, \quad \boldsymbol{\Lambda}_{21} = \begin{pmatrix} \varepsilon_{0,0} & \varepsilon_{0,1} & \cdots & \varepsilon_{0,m-1} & \varepsilon_{0,m} \\ \varepsilon_{1,0} & \varepsilon_{1,1} & \cdots & \varepsilon_{1,m-1} & \varepsilon_{1,m} \\ \vdots & \vdots & \cdots & \vdots & \vdots \\ \varepsilon_{m-2,0} & \varepsilon_{m-2,1} & \cdots & \varepsilon_{m-2,m-1} & \varepsilon_{m-2,m} \\ 0 & 0 & \cdots & 0 & 0 \\ -1 & 1 & \cdots & (-1)^{m-1} & (-1)^{m} \end{pmatrix},$$

$$\boldsymbol{\Lambda}_{22} = \begin{pmatrix} \alpha_{0,0} & \alpha_{0,1} & \cdots & \alpha_{0,m-1} & \alpha_{0,m} \\ \alpha_{1,0} & \alpha_{1,1} & \cdots & \alpha_{1,m-1} & \alpha_{1,m} \\ \vdots & \vdots & \vdots & \vdots & \vdots \\ \alpha_{m-2,0} & \alpha_{m-2,1} & \cdots & \alpha_{m-2,m-1} & \alpha_{m-2,m} \\ 1 & 1 & \cdots & 1 & 1 \\ 0 & 0 & \cdots & \frac{n}{2\eta_\infty^2} c_i \prod_{o=-1}^{2} (m+o-1) & \frac{n}{2\eta_\infty^2} c_i \prod_{o=-1}^{2} (m+o) \end{pmatrix},$$

$$\mathbf{b_1} = \begin{pmatrix} 0 & 0 & 0 & 0 & 0 & 0 & \cdots & 0 & \frac{\eta_\infty}{2} & 0 \end{pmatrix}^T, \quad \mathbf{b_2} = (\,0 \quad 0 \quad 0 \quad 0 \quad 0 \quad 0 \quad \cdots \quad 0 \quad 0 \quad 0\,)^T,$$

$$\mathbf{c} = \left\{\text{span}\{c_j\}\right\}, \quad \tilde{\mathbf{c}} = \left\{\text{span}\{c_i\, c_j\}, \text{span}\{d_i\, d_j\}\right\}, \quad \bar{\mathbf{c}} = \left\{\text{span}\{c_i\, c_j\, c_k\}, \text{span}\{d_i\, d_j\, d_k\}\right\},$$

$$\check{\mathbf{c}} = \left\{\text{span}\{c_i\, d_j\}\right\}, \quad \boldsymbol{\Phi}_{\mathbf{f}} = \{\Omega_{i,\,j,\,r}\}, \quad \boldsymbol{\Theta}_{\mathbf{f}} = \{\kappa_{i,\,j,\,k,\,r}\}, \quad \boldsymbol{\Gamma}_{\mathbf{f}} = \{e_{i,\,j,\,r}\},$$

$$\omega_{j,r} = \frac{1}{\eta_\infty} \langle \frac{8}{\eta_\infty^2} (1+K) P_j'''(\xi) + (1-\zeta) P_j''(\xi) - (1-\zeta)\xi P_j''(\xi) - 2M P_j'(\xi), P_r(\xi) \rangle \tag{14}$$

$$\epsilon_{j,r} = \frac{2K}{\eta_\infty} \langle P_j'(\xi), P_r(\xi) \rangle, \quad \varepsilon_{j,r} = -\frac{4K\zeta}{\eta_\infty^2} \langle P_j''(\xi), P_r(\xi) \rangle, \tag{15}$$

$$\alpha_{i,j} = \langle \frac{1}{\eta_\infty^2} (4+2K) P_j''(\xi) + (1-\zeta)\left(P_j'(\xi) + \xi P_j'(\xi)\right) + (2K\zeta + \xi + 1) P_j(\xi), P_r(\xi) \rangle, \tag{16}$$

$$\Omega_{i,\,j,\,r} = \frac{4\zeta}{\eta_\infty^2} \left[\langle P_i(\xi)\, P_j''(\xi) - P_i'(\xi) P_j'(\xi), P_r(\xi) \rangle \right], \tag{17}$$

$$\kappa_{i,\,j,\,k,\,r} = \frac{8\zeta\beta}{\eta_\infty^3} \left[2\langle P_i(\xi) P_j''(\xi) P_j'(\xi), P_r(\xi) \rangle - \langle P_i(\xi) P_j(\xi) P_j'''(\xi), P_r(\xi) \rangle \right], \tag{18}$$

$$e_{i,\,j,\,r} = \frac{2\zeta}{\eta_\infty} \langle P_i(\xi) P_j'(\xi) - P_j(\xi) P_i'(\xi), P_r(\xi) \rangle. \tag{19}$$

Fathy *et al.,* [20-24] developed theorems and lemmas to compute the terms in Eq. **Error! Reference source not found.** to Eq. **Error! Reference source not found.**. There are (2n+2) unknowns in the nonlinear system (20). This system was approached using the Newton method. The

unknowns $\{c_j\}_{j=0}^{n}$ and $\{d_j\}_{j=0}^{n}$ may be determined once the system was solved. Finally, the inverse transformation $\xi = 2\eta/\eta_\infty - 1$ is employed to find the problem's solutions. Some of the obtained solutions are listed in Table 1.

Table 1
Certain gained asymptotic results at $n = 15$

	Solutions
$M = 1,\ \zeta = 1, \beta = 0.2$ $K = 1,\ n = 0.5$	$f(\eta) = \eta - 0.369\eta^2 + 0.06165020374377372 4\eta^3 - 0.00174\eta^4 - 0.0010578\eta^5 + 0.000211\eta^6 - 0.000032\eta^7 + 0.0000034\eta^8 + 0.000001076\eta^9 - 5.98 \times 10^{-7}\eta^{10} + 1.3 \times 10^{-7}\eta^{11} - 1.6 \times 10^{-8}\eta^{12} + 1.27 \times 10^{-9}\eta^{13} - 5.57 \times 10^{-11}\eta^{14} + 1.07 \times 10^{-12}\eta^{15}$
	$g(\eta) = 0.369004 - 0.1398\eta - 0.00615 + 0.004805702143322993 5\eta^3 + 0.001905\eta^4 - 0.000634\eta^5 - 0.00004175085899481127 4\eta^6 + 0.000031007\eta^7 - 2.53 \times 10^{-7}\eta^8 - 0.00000138244435548810 6\eta^9 + 2.43 \times 10^{-7}\eta^{10} - 8.36 \times 10^{-9}\eta^{11} - 2.423 \times 10^{-9}\eta^{12} + 3.73 \times 10^{-10}\eta^{13} - 2.24 \times 10^{-11}\eta^{14} + 5.28 \times 10^{-13}\eta^{15}$
$M = 1,\ \zeta = 1, \beta = 0.1$ $K = 4,\ n = 0.5$	$f(\eta) = \eta - 0.259\eta^2 + 0.0303\eta^3 - 0.000678\eta^4 - 0.0001877177903757711 8\eta^5 + 0.0000108\eta^6 + 5.648 \times 10^{-7}\eta^7 + 8.288 \times 10^{-8}\eta^8 - 1.15 \times 10^{-8}\eta^9 - 5.17 \times 10^{-9}\eta^{10} + 1.3 \times 10^{-9}\eta^{11} - 1.31 \times 10^{-10}\eta^{12} + 6.84 \times 10^{-12}\eta^{13} - 1.611 \times 10^{-13}\eta^{14} + 7.5 \times 10^{-16}\eta^{15}$
	$g(\eta) = 0.25972 - 0.0779\eta - 0.002164\eta^2 + 0.002547413230849712 3\eta^3 + 0.000031\eta^4 - 0.0000853\eta^5 + 0.0000059\eta^6 + 0.000001056\eta^7 - 1.4 \times 10^{-7}\eta^8 - 1.426027240013162 \times 10^{-9}\eta^9 + 3.6 \times 10^{-10}\eta^{10} + 2.3 \times 10^{-10}\eta^{11} - 4.5 \times 10^{-11}\eta^{12} + 3.6 \times 10^{-12}\eta^{13} - 1.3 \times 10^{-13}\eta^{14} + 2.1 \times 10^{-15}\eta^{15}$

5. Results and Discussion

The flow horizontal velocity and micro-rotation velocity are graphically displayed for varied valuation of the magnetic parameter M, elasticity number β and material parameter K, as well as the skin friction for various non-Newtonian components. Tables 2, 3 and 4 show good agreement with prior published results for skin friction in the lack of a magnetic field, ensuring accuracy of our work.

Table 2
The skin friction coefficient at $\beta = 0, \zeta = 1, M = 0$ and $n = 0$ for distinct values of K

	Skin Friction $= -\boldsymbol{\zeta^{-0.5}}[\mathbf{1} + (\mathbf{1} - \boldsymbol{n})\boldsymbol{K}]\, \boldsymbol{f''(0)}$			
$\boldsymbol{K}$	Ishak *et al.,* [25]	D.A. Aldawody [13]	M. Qasim [26]	Present results
0	1	1	1	1
1	1.3679	1.3679	1.367872	1.36799
2	1.6213	1.6213	1.621225	1.62158
4	2.0042	2.0043	2.004133	2.00544

Table 3
The skin friction coefficient at $\beta = 0, \zeta = 1, M = 0$ and $n = 0.5$ for distinct values of K

	Skin Friction $= -\boldsymbol{\zeta^{-0.5}}[\mathbf{1} + (\mathbf{1} - \boldsymbol{n})\boldsymbol{K}]\, \boldsymbol{f''(0)}$			
$\boldsymbol{K}$	Ishak [25]	D.A. Aldawody [13]	M. Qasim [26]	Present results
0	1	1	1	1
1	1.2247	1.2247	1.224741	1.22481
2	1.4142	1.4142	1.414218	1.41447
4	1.7343	1.7343	1.732052	1.73329

Table 4
Comparison of $-\zeta^{-0.5}[1+(1-n)K]\,f''(0)$ at $K=0, \zeta=1, M=0$ and $n=0$ for different values of β.

$\boldsymbol{\beta}$	Sadeghy *et al.,* [27]	Subahs [2]	Swati [10]	Present results
0	1	0.999962	0.999963	1.000007
0.2	1.0549	1.051948	1.051949	1.053371
0.4	1.10084	1.101850	1.101851	1.100163
0.6	1.15016	1.150163	1.150162	1.147450
0.8	1.19872	1.196692	1.196693	1.176135

According to Figures 2(a) and 2(b), when the magnetic field M is raised, increasing the peak value of angular velocity while dropping in horizontal velocity occurs. The Lorentz force is a drag force that causes the flow velocity to shrink and the thickness of boundary layer to decrease owing to the applicable transverse magnetic field.

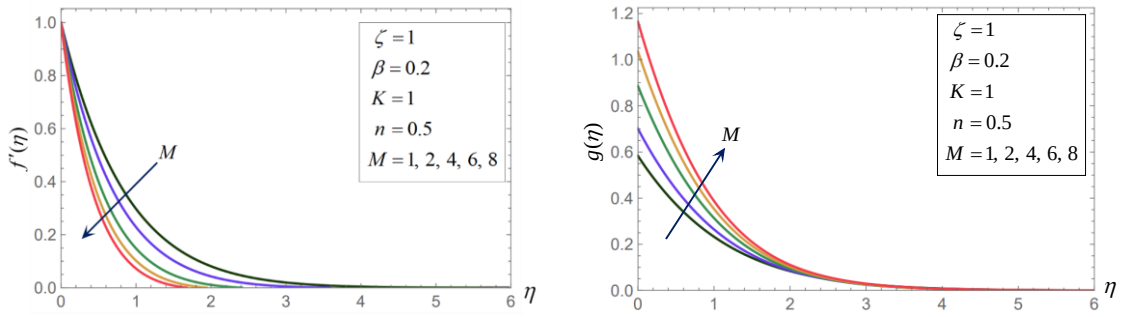

(a) (b)

Fig. 2. (a) The impact of M on the velocity and (b) The effect of M on the microrotation

As soon as the micro-rotation viscosity is diminished, the conservation equation of linear momentum no longer depends on microstructures. The micro-rotation s is the material parameter K in its dimensionless formulation. The microstructure's viscosity governs its angular rotation. To illustrate this, the maximum angular velocity lowers, the boundary layer depth and the horizontal velocity field increase, as seen in Figures 3(a) and 3(b), when the material parameter K rises apart from the surface but the reverse happens close to the surface.

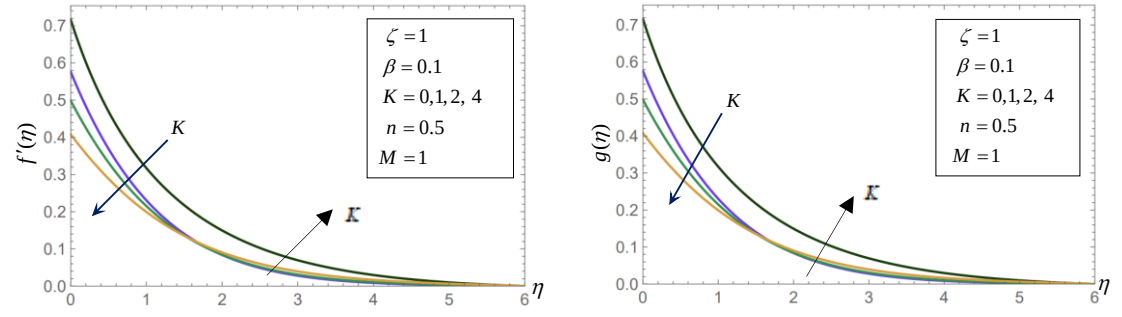

(a) (b)

Fig. 3. The impact of K on (a) the velocity and (b) Micro-rotation profile at different K

The elasticity number β is calculated by dividing the time it takes for a material to relax after being subjected to stress or distortion by normal time scale of a trial. In Figure 4(a), the velocity decreases as the elasticity amplifies. Naturally, with rich elasticity values, material nigh a solid state where elasticity is dominant, slowing the flow rate down. A raise in the highest angular velocity may be seen in Figure 4(b).

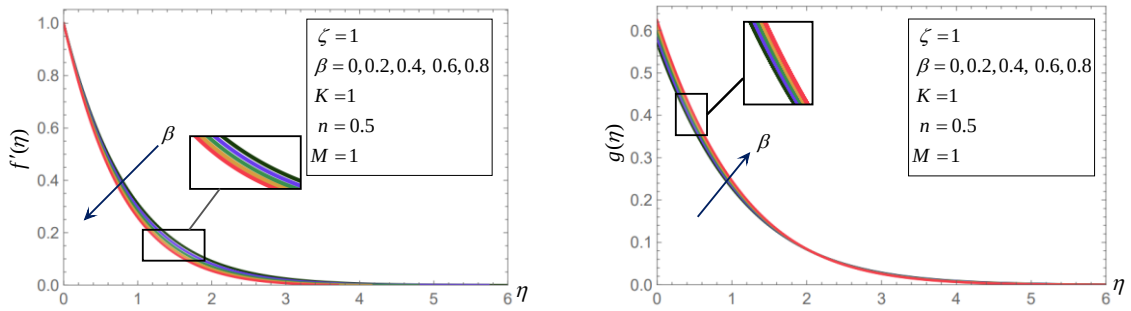

(a) (b)

Fig. 4. The impact of β on (a) the velocity and (b) Micro-rotation profile at different β

There is a drop in the horizontal velocity at ζ =1 when the flow enters steady state as observed in Figure 5(a) while Figure 5(b) shows a rise in maximum angular velocity as time goes on.

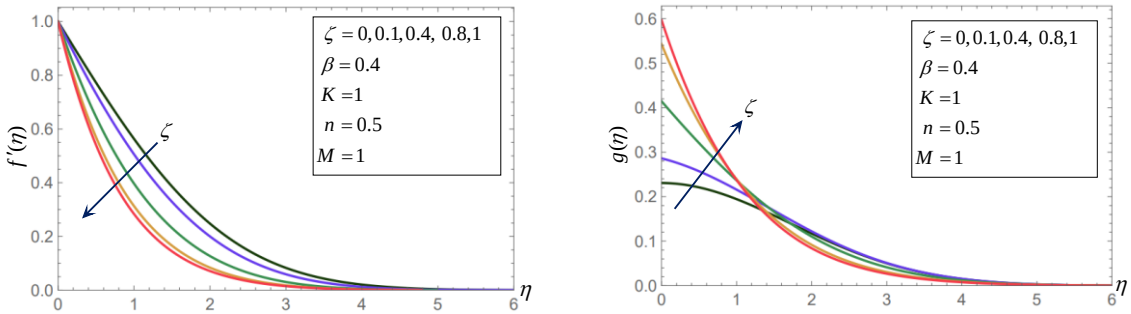

(a) (b)

Fig. 5. (a) The impact of ζ on the velocity and (b) Micro-rotation profile at different ζ

Table 5 shows numerical data for skin friction for weak and strong fluids in the existence of a magnetic field at different levels of elasticity number β. The table displays the results when the micro-polar effect is absent $(K = 0)$ and when it is present $(K = 1)$. The info confesses that as elasticity β raises, skin friction increases in all circumstances. In the absence of material parameter $(K = 0)$, skin friction is same for weak and strong fluids.

Table 5
The impact of β on $-f''(0)$ at $\zeta = 1, M = 1$

	$K = 0$		$K = 1$	
β	$n = 0$	$n = 0.5$	$n = 0$	$n = 0.5$
0	1.414216	1.414216	0.971142	1.1376808
0.2	1.450241	1.450241	0.996688	1.1662131
0.4	1.485725	1.485725	1.021871	1.1942605
0.8	1.555044	1.555044	1.071112	1.2489034

The skin friction of the weak fluid is made lower than that of the strong fluid when the material parameter is present $(K = 1)$. In practice, skin friction is crucial in several manufacturing processes, such as cooling operations. Low friction indicates less drag force is needed to pull a moving surface, or less power is required to accomplish the specified drag velocity.

Table 6 demonstrates the impression of the magnetic parameter M on Micropolar fluid in both lack and presence of the elasticity. When the elasticity parameter $\beta = 0.2$ is present than when elasticity parameter $\beta = 0$ is present, skin friction is greater. When magnetic M rises, skin friction also enhances. Due to Lorentz drag caused by the magnetic field, the shift from a laminar to a turbulent flow was delayed.

Table 6
The impact of M on $-f''(0)$ at $\zeta = 1, K = 1$

	$\boldsymbol{\beta = 0}$		$\boldsymbol{\beta = 0.2}$	
$\boldsymbol{M}$	$n = 0$	$n = 0.5$	$n = 0$	$n = 0.5$
0	0.68520322	0.81800377	0.72140338	0.85931319
1	0.97114272	1.13768086	0.99668815	1.16621319
2	1.19394809	1.37859799	1.21469879	1.40147034
4	1.54945586	1.75457035	1.56545806	1.77192531

Table 7 depicts the echo of material parameter on skin friction in existence/absence of magnetic field. Magnetic field influences skin friction, although not as much as it does without one (explained before physically). As material parameter rises, skin friction lessens. Vortex expansion leads to a growth in velocity and a loss in skin friction as the material parameter rises.

Table 7
The impact of K on $-f''(0)$ at $\zeta = 1, \beta = 0.1$

	$\boldsymbol{M = 0}$		$\boldsymbol{M = 1}$	
$\boldsymbol{K}$	$n = 0$	$n = 0.5$	$n = 0$	$n = 0.5$
0	1.02653621	1.02653621	1.43229609	1.43229609
1	0.70342601	0.83882087	0.98395958	1.15200734
2	0.55701139	0.72772090	0.78017038	0.99726838
4	0.41530962	0.59716787	0.58080459	0.81615734

6. Conclusions

The Legendre-Galerkin method is used in this study to inspect the impact of magnetic field on boundary layer flow in Maxwell fluid over an unsteady stretched surface. A comparison was made with earlier released studies, and the info is very similar. It is investigated the impacts of the preceding factors on flow, skin friction and micro-rotation. The following points are discovered:

i. When magnetic field is increased, Lorentz force is produced, which lessens flow velocity. Hence, depth of the boundary layer is lessened. It also raises angular velocity's maximum value.
ii. The velocity and the highest angular velocity rise when the material and the elasticity parameters are increased.

When the elasticity number and the magnetic field are increased, or when the material parameter is decreased, the skin friction increases.

Acknowledgement
This research was not funded by any grant.

References
[1] Becher, Paul. "A review of:"Polymers as Rheology Modifiers (ACS Symposium Series 462)": Schulz, DN; Glass. JE, Eds.; American Chemical Society: Washington, 1991. pp. xii+ 345. $84.95." *JOURNAL OF DISPERSION SCIENCE AND TECHNOLOGY* 13, no. 5 (1992): 582-582. https://doi.org/10.1080/01932699208943337
[2] Subhas Abel, M., Jagadish V. Tawade, and Mahantesh M. Nandeppanavar. "MHD flow and heat transfer for the upper-convected Maxwell fluid over a stretching sheet." *Meccanica* 47 (2012): 385-393. https://doi.org/10.1007/s11012-011-9448-7
[3] Sarpkaya, Turgut. "Flow of non-Newtonian fluids in a magnetic field." *AIChE Journal* 7, no. 2 (1961): 324-328. https://doi.org/10.1002/aic.690070231
[4] Hayat, T., and M. Qasim. "Influence of thermal radiation and Joule heating on MHD flow of a Maxwell fluid in the presence of thermophoresis." *International Journal of Heat and Mass Transfer* 53, no. 21-22 (2010): 4780-4788. https://doi.org/10.1016/j.ijheatmasstransfer.2010.06.014
[5] Sadeghy, Kayvan, Amir-Hosain Najafi, and Meghdad Saffaripour. "Sakiadis flow of an upper-convected Maxwell fluid." *International Journal of Non-Linear Mechanics* 40, no. 9 (2005): 1220-1228. https://doi.org/10.1016/j.ijnonlinmec.2005.05.006
[6] Hayat, T., C. Fetecau, and M. Sajid. "On MHD transient flow of a Maxwell fluid in a porous medium and rotating frame." *Physics letters A* 372, no. 10 (2008): 1639-1644. https://doi.org/10.1016/j.physleta.2007.10.036
[7] Aliakbar, V., A. Alizadeh-Pahlavan, and K. Sadeghy. "The influence of thermal radiation on MHD flow of Maxwellian fluids above stretching sheets." *Communications in Nonlinear Science and Numerical Simulation* 14, no. 3 (2009): 779-794. https://doi.org/10.1016/j.cnsns.2007.12.003
[8] Singh, Vijendra, and Shweta Agarwal. "MHD flow and heat transfer for Maxwell fluid over an exponentially stretching sheet with variable thermal conductivity in porous medium." *Thermal science* 18, no. suppl. 2 (2014): 599-615. https://doi.org/10.2298/TSCI120530120S
[9] Tey, Wah Yen, Yutaka Asako, Nor Azwadi Che Sidik, and Rui Zher Goh. "Governing equations in computational fluid dynamics: Derivations and a recent review." *Progress in Energy and Environment* (2017): 1-19.
[10] Mukhopadhyay, Swati, M. Golam Arif, and M. Wazed Ali Pk. "Effects of transpiration on unsteady MHD flow of an upper convected Maxwell (UCM) fluid passing through a stretching surface in the presence of a first order chemical reaction." *Chinese Physics B* 22, no. 12 (2013): 124701. https://doi.org/10.1088/1674-1056/22/12/124701
[11] Shateyi, Stanford. "A new numerical approach to MHD flow of a Maxwell fluid past a vertical stretching sheet in the presence of thermophoresis and chemical reaction." *Boundary Value Problems* 2013 (2013): 1-14. https://doi.org/10.1186/1687-2770-2013-196
[12] Lukaszewicz, Grzegorz. *Micropolar fluids: theory and applications*. Springer Science & Business Media, 2012.
[13] Aldawody, D. A., and E. M. A. Elbashbeshy. "Heat transfer over an unsteady stretching surface in a micropolar fluid in the presence of magnetic field and thermal radiation." *Canadian Journal of Physics* 89, no. 3 (2011): 295-298. https://doi.org/10.1139/P11-027
[14] Shit, G. C., R. Haldar, and A. Sinha. "Unsteady flow and heat transfer of a MHD micropolar fluid over a porous stretching sheet in the presence of thermal radiation." *Journal of Mechanics* 29, no. 3 (2013): 559-568. https://doi.org/10.1017/jmech.2013.33
[15] Haque, Md Ziaul, Md Mahmud Alam, M. Ferdows, and A. Postelnicu. "Micropolar fluid behaviors on steady MHD free convection and mass transfer flow with constant heat and mass fluxes, joule heating and viscous dissipation." *Journal of King Saud University-Engineering Sciences* 24, no. 2 (2012): 71-84. https://doi.org/10.1016/j.jksues.2011.02.003
[16] Aurangzaib, A. R. M. Kasim, N. F. Mohammad, and Sharidan Shafie. "Unsteady MHD mixed convection flow of a micropolar fluid along an inclined stretching plate." *Heat Transfer—Asian Research* 42, no. 2 (2013): 89-99. https://doi.org/10.1002/htj.21034
[17] Sharafatmandjoor, S., and CS Nor Azwadi. "Effect of viscous and thermal forcings on dynamical features of swimming of microorganisms in nanofluids." *Journal of Advanced Research in Fluid Mechanics and Thermal Sciences* 17, no. 1 (2016): 18-27.
[18] Kianpour, Ehsan, Nor Azwadi Che Sidik, Seyyed Muhammad Hossein Razavi Dehkordi, and Siti Nurul Akmal Yusof. "Numerical Simulation of Steady and Unsteady Flow and Entropy Generation by Nanofluid Within a Sinusoidal Channel." *Journal of Advanced Research in Fluid Mechanics and Thermal Sciences* 89, no. 2 (2022): 25-42. https://doi.org/10.37934/arfmts.89.2.2542

[19] Sharafatmandjoor, Shervin. "Effects of The Optimal Imposition of Viscous and Thermal Forces on Spectral Dynamical Features of Swimming of a Microorganism in Nanofluids." *Journal of Advanced Research in Micro and Nano Engineering* 8, no. 1 (2022): 1-8.
[20] Fathy, Mohamed. "Legendre-Galerkin method for the nonlinear Volterra-Fredholm integro-differential equations." In *Journal of Physics: Conference Series*, vol. 2128, no. 1, p. 012036. IOP Publishing, 2021. https://doi.org/10.1088/1742-6596/2128/1/012036
[21] El-Gamel, Mohamed, M. S. El-Azab, and Mohamed Fathy. "An efficient technique for finding the eigenvalues and the eigenelements of fourth-order Sturm-Liouville problems." *SeMA Journal* 74 (2017): 37-56. https://doi.org/10.1007/s40324-016-0079-8
[22] El-Gamel, M., M. S. El-Azab, and M. Fathy. "The numerical solution of sixth order boundary value problems by the legendre-galerkin method." *Acta Univ. Apulensis Math. Inform* 40 (2014): 145-165. https://doi.org/10.17114/j.aua.2014.40.13
[23] Fathy, Mohamed, Mohamed El-Gamel, and M. S. El-Azab. "Legendre–Galerkin method for the linear Fredholm integro-differential equations." *Applied Mathematics and Computation* 243 (2014): 789-800. https://doi.org/10.1016/j.amc.2014.06.057
[24] El-Gamel, Mohamed, Galal I. El-Baghdady, and Mahmoud Abd El-Hady. "Highly efficient method for solving parabolic PDE with nonlocal boundary conditions." *Applied Mathematics* 13, no. 2 (2022): 101-119. https://doi.org/10.4236/am.2022.132009
[25] Ishak, Anuar, Roslinda Nazar, and I. Pop. "Hydromagnetic flow and heat transfer adjacent to a stretching vertical sheet." *Heat and Mass Transfer* 44, no. 8 (2008): 921-927. https://doi.org/10.1007/s00231-007-0322-z
[26] Qasim, Muhammad, Ilyas Khan, and Sharidan Shafie. "Heat transfer in a micropolar fluid over a stretching sheet with Newtonian heating." *PLOS one* 8, no. 4 (2013): e59393. https://doi.org/10.1371/journal.pone.0059393
[27] Sadeghy, Kayvan, Hadi Hajibeygi, and Seyed-Mohammad Taghavi. "Stagnation-point flow of upper-convected Maxwell fluids." *International journal of non-linear mechanics* 41, no. 10 (2006): 1242-1247. https://doi.org/10.1016/j.ijnonlinmec.2006.08.005